blood®
Regular Article

HEMATOPOIESIS AND STEM CELLS

Regeneration after blood loss and acute inflammation proceeds without contribution of primitive HSCs

Clara M. Munz,[1] Nicole Dressel,[1] Minyi Chen,[2] Tatyana Grinenko,[3] Axel Roers,[1,2] and Alexander Gerbaulet[1]

[1]Institute for Immunology, Faculty of Medicine, TU Dresden, Dresden, Germany; [2]Institute for Immunology, Heidelberg University Hospital, Heidelberg, Germany; and [3]Institute for Clinical Chemistry and Laboratory Medicine, Faculty of Medicine, TU Dresden, Dresden, Germany

KEY POINTS

- **Cumulative recording of proliferation and differentiation in situ shows that primitive HSCs are not activated by inflammation or blood loss.**

Hematopoietic stem cells (HSCs) are the ultimate source of blood and immune cells, and transplantation reveals their unique potential to regenerate all blood lineages lifelong. HSCs are considered a quiescent reserve population under homeostatic conditions, which can be rapidly activated by perturbations to fuel blood regeneration. In accordance with this concept, inflammation and loss of blood cells were reported to stimulate the proliferation of HSCs, which is associated with a decline in their transplantation potential. To investigate the contribution of primitive HSCs to the hematopoietic stress response in the native environment, we use fate mapping and proliferation tracking mouse models. Although primitive HSCs were robustly activated by severe myeloablation, they did not contribute to the regeneration of mature blood cells in response to prototypic hematopoietic emergencies, such as acute inflammation or blood loss. Even chronic inflammatory stimulation, which triggered vigorous HSC proliferation, only resulted in a weak contribution of HSCs to mature blood cell production. Thus, our data demonstrate that primitive HSCs do not participate in the hematopoietic recovery from common perturbations and call for the reevaluation of the concept of HSC-driven stress responses.

Introduction

The hematopoietic system continuously generates enormous numbers of mature blood cells,[1] and its output can be substantially accelerated by blood loss or infections. Hematopoietic stem cells (HSCs), which reside at the top of the hematopoietic hierarchy, give rise to mature blood cells via diverse progenitor intermediates. Upon transplantation, only this somatic stem cell population is able to reconstitute all blood cell lineages lifelong, which is the basis for therapeutic or experimental HSC transplantation.[2,3] Although hematopoiesis after transplantation is driven by a few HSC clones,[4-6] fate tracking of native hematopoiesis in adult mice revealed only rare but continuous and polyclonal HSC differentiation.[6-9] Moreover, murine HSCs remain largely quiescent in adult steady-state hematopoiesis.[10,11] A recent study revealed the enormous regenerative capacity of progenitor populations, which despite lack of long-term transplantation potential, contribute lifelong to native hematopoiesis.[12] Models of HSC depletion further emphasize the robustness of blood formation in the absence of HSCs.[13,14] Currently, HSCs are perceived as a quiescent reserve population, which is essential to boost blood cell output in situations of acute demand.[15-17] In response to infection or blood loss, HSCs are thought to be activated via pattern recognition and cytokine receptors and participate in hematopoietic stress responses, ultimately resulting in a gradual loss of their transplantation potential (as reviewed previously[18]).

Here, we used mouse models of fate and proliferation tracking to study HSC activity in response to prototypic hematopoietic perturbations. We found that acute inflammatory signaling resulting in massively enhanced blood cell output was reflected in little, if any, increase in the contribution of primitive HSCs. Similarly, hematopoietic stress caused by the extensive depletion of mature blood cells did not trigger accelerated stem cell proliferation or differentiation. Only pharmacological or irradiation-induced severe depletion of hematopoietic progenitors triggered a robust plus in HSC activity. We thus argue against primitive HSCs constituting a reserve population that boosts hematopoiesis in response to acute inflammation or blood cell loss and propose that they may only be needed in situations of extreme distress.

Methods

Mice

All animal experiments were performed in accordance with institutional guidelines and the German Law for Protection of Animals, approved by the Landesdirektion Dresden (TVV 91/2017). Mice were housed in individually ventilated cages under a specific pathogen-free environment at the Experimental

Center of the Medical Faculty, TU Dresden. *R26*$^{rtTA/rtTA}$/*Col1A1*$^{H2B\text{-}GFP/H2B\text{-}GFP}$[19] mice were induced with doxycycline (DOX, 2 g/kg) via chow (Ssniff Spezialdiäten) for 1 to 2 weeks ad libitum. *Fgd5*$^{ZsGreen:CreERT2/wt}$/*R26*$^{LSL\text{-}tdRFP/LSL\text{-}tdRFP}$[20,21] mice were induced by oral gavage of tamoxifen (TAM, 0.2 mg/g body weight [BW]) twice 3 to 4 days apart. Fate mapping and transplantation data from *Fgd5*$^{ZsGreen:CreERT2}$/*R26*$^{LSL\text{-}tdRFP}$ mice shown in Figure 1C-D and supplemental Figure 2, which is available on the *Blood* website, and 5-fluorouracil (5-FU) perturbation data shown in Figure 1G-P and supplemental Figure 3C-G was previously published.[22] 5-FU (150 µg/g BW; Applichem) was administered via IV injection. Whole-body irradiation was performed using an Yxlon Maxi Shot X-ray tube at a dose of 2 Gy. Recombinant human granulocyte-colony stimulating factor (G-CSF; filgrastim) (0.3 µg/g BW; Neupogen, Amgen) was administered by subcutaneous (SC) injection on 5 consecutive days. Polyinosinic:polycytidylic acid (pI:C; 5 µg/g BW; Invivogen) was administered via intraperitoneal (IP) injection either 1 ("single" protocol) or 8 times ("repetitive" protocol, 2 injections per week). Lipopolysaccharide (LPS) (from *Escherichia coli* O111:B4, Invivogen; 35 µg per mouse in 2 out of 4 experiments and adjusted to 1.4 µg/g BW in the remaining experiments) was IP injected. Rabbit antimouse thrombocyte serum (50 to 70 µL per mouse in a total volume of 150 µL; effective dosage was pre-titrated for each batch of serum; WAK-Chemie Medical GmbH) or mock serum was administered IP either once ("acute" protocol) or 7 times ("chronic" protocol, injection every other day). Phenylhydrazine (PHZ, 40 µg/g BW; Sigma-Aldrich) was IP injected twice on 2 consecutive days.

Cell preparation

Whole bone marrow (BM) cells were extracted by crushing long bones with mortar and pestle using phosphate-buffered saline (PBS), 2% fetal calf serum (FCS), and 2 mM EDTA and filtering twice after erythrocyte lysis in hypotonic NH_4Cl buffer. Hematopoietic lineage-positive (lin^+) cells were depleted from samples with the lineage cell depletion kit (Miltenyi Biotec).

Peripheral blood (PB) was drawn into glass capillaries by retrobulbar puncture directly into EDTA-coated tubes (Sarstedt). For the identification of red fluorescent protein–positive (RFP^+) platelets and erythrocytes, 1 to 2 µL of whole blood was mixed with PBS, 2% FCS, and 2 mM EDTA and incubated with monoclonal antibodies. For PB leukocyte analysis, erythrocyte lysis in hypotonic NH_4Cl buffer was performed twice for 5 minutes before cells were stained with monoclonal antibodies. For hemograms, blood was diluted 1:5 in an isotonic NaCl solution and analyzed on an XT-2000i Vet analyzer (Sysmex).

Spleen cell suspensions were prepared by mashing spleens using PBS, 2% FCS, and 2 mM EDTA through a 100 µm mesh and subsequent erythrocyte lysis in hypotonic NH_4Cl buffer.

Peritoneal cells were obtained by flushing the peritoneal cavity with 4 mL PBS, 2% FCS, and 2 mM EDTA and filtering the aspirate through a 100 µm mesh.

Flow cytometry

Cell suspensions from BM, spleen, peritoneal lavage, or PB samples were stained with antibodies (supplemental Table 1) in PBS, 2% FCS, and 2 mM EDTA for 30 to 40 minutes, washed twice, and analyzed on either FACS Canto, ARIA II SORP, Aria II, ARIA III (all from BD Biosciences, Heidelberg, Germany) or MACSquant (Miltenyi Biotec) flow cytometers. FlowJo V9.9 and V10 software (Tree Star) was used for data analysis, and gates (supplemental Figure 1A-D) were set using Fluorescence-Minus-One controls. Gating of RFP^+ cells was guided by negative (Cre^- animal) and positive (germ line STOP-excised *R26*^{tdRFP} mouse with ubiquitous RFP expression) controls. Absolute numbers of lin^- BM cells were determined using a MACSquant flow cytometer.

Measurement of PB cytokine concentrations

PB samples were centrifuged (10 minutes, 1000*g*) within 30 minutes of blood collection. Plasma supernatants were frozen at −20 °C until analysis. Plasma cytokine concentration was measured using the LEGENDplex Mouse Inflammation Panel (13-plex, BioLegend), according to the manufacturer's instructions. Flow cytometric analysis was performed on a MACSquant flow cytometer; data analysis was performed by the LEGENDplex Data Analysis Software Suite.

Data normalization and statistics

RFP label propagation data from BM and PB populations of induced *Fgd5*$^{ZsGreen:CreERT2}$/*R26*$^{LSL\text{-}tdRFP}$ mice was normalized to the label in HSCs with a high surface expression of CD201 (EPCR) and Sca-1 (ES HSCs) of the same animal. The percentage of label increase caused by the stress response was calculated by subtracting the normalized arithmetic mean of label in control animals from the normalized label in a treated specimen (supplemental Figure 3F). The percentage of label increase was summarized in radar charts (Figures 1P, 2P, and 3M). Gray shaded areas provide an estimate of data variation (standard deviation calculated from unperturbed control animals, n = 41 from 8 experiments (supplemental Figure 3G-H).

Histone 2b-green fluorescent protein (H2B-GFP) label retention data from *R26*^{rtTA}/*Col1A1*$^{H2B\text{-}GFP}$ mice was normalized to express the number of additional divisions in perturbed vs control animals by subtracting the H2B-GFP mean fluorescence intensity of a specific animal and population from the corresponding mean fluorescence intensity thereof in control animals (supplemental Figure 3D-E). For more details on data normalization, refer to supplemental Methods.

All graphs shown in main or supplementary figures are designed with the following properties: individual mice are shown; boxplots show medians, lower, and upper quartiles; dotted lines represent means of untreated controls; bar graphs show means; significance between perturbed and control mice was calculated by an unpaired Student *t* test except for supplemental Figures 2D, 3B, and 4R, in which a 1-way analysis of variance with Tukey's post-hoc test was applied (*$P \geq .05$; **$P \geq .01$, ***$P \geq .001$, nonsignificant differences are not indicated).

Results

Fate mapping and proliferation tracking of perturbed hematopoiesis

To investigate the contribution of primitive HSCs to hematopoietic stress responses, we used the *Fgd5*$^{ZsGreen:CreERT2}$/*R26*$^{LSL\text{-}tdRFP}$ fate mapping mouse model,[20,21] in which TAM

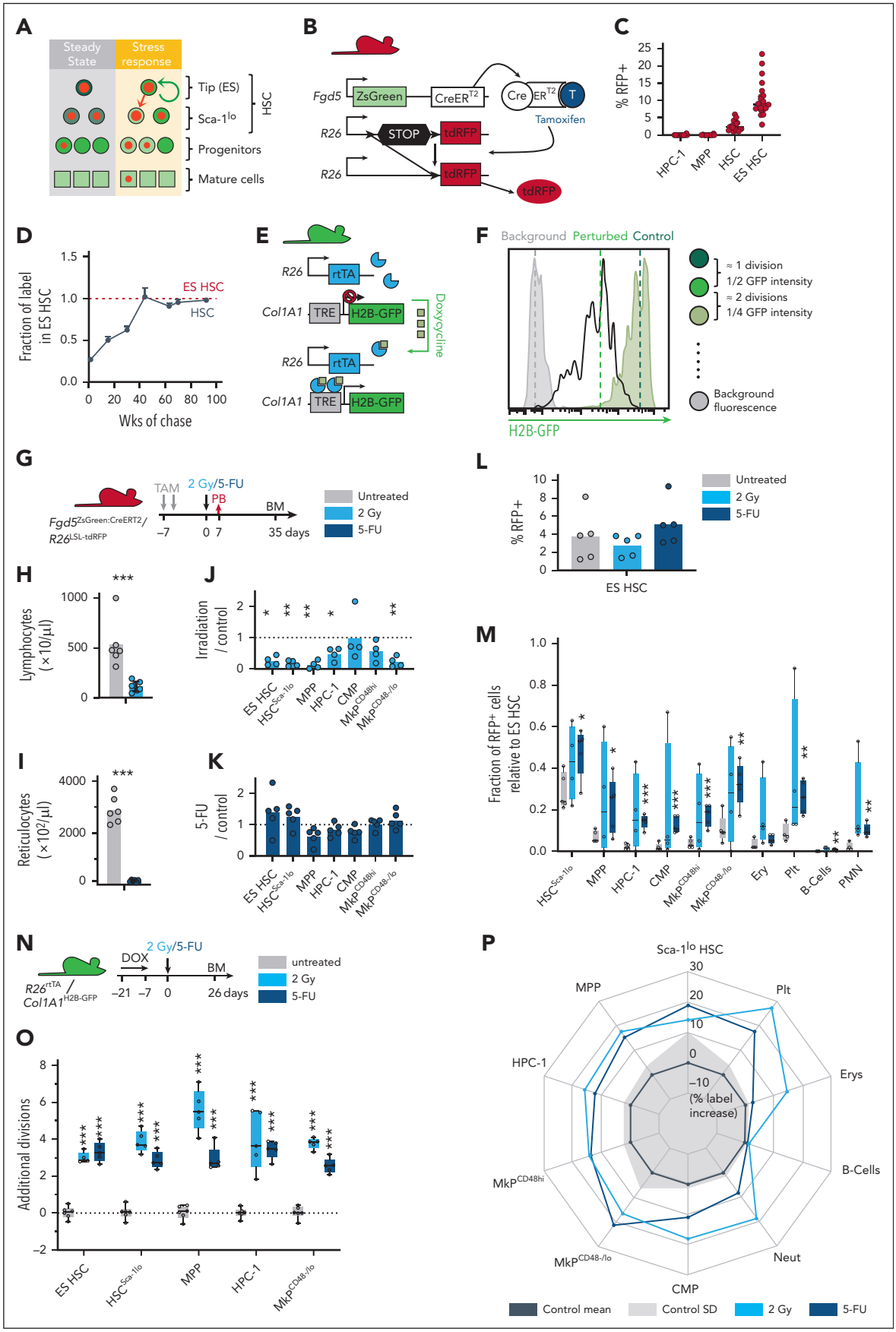

Figure 1.

selectively induces inheritable RFP expression in adult immunophenotypic (lin$^-$ Sca-1$^+$ Kit$^+$ [LSK] CD48$^{-/lo}$ CD150$^+$) (Figure 1A-C; see supplemental Figure 1A-D for gating) HSCs.[22] As previously established,[22] this model preferentially labels a small subpopulation of HSCs at the apex of the hematopoietic hierarchy identified by high surface expression of CD201 (EPCR) and Sca-1 (termed "ES HSCs" or "tip" HSCs). ES HSCs overlapped with other HSC subsets known for high transplantation potential, namely Sca-1^{hi} HSCs[23] and Fgd5$^+$ HSCs[21,24] (supplemental Figure 2A-C) and expressed the highest levels of Fgd5 reporter (supplemental Figure 2D). In addition, ES HSCs performed better upon transplantation than HSCs, which were solely selected based on Fgd5 reporter expression (supplemental Figure 2E-G). To monitor the propagation of label from ES HSCs to their progeny and to adjust for the interindividual variability of labeling efficiency, we calculated the fraction of ES HSC–derived label in each cell population under investigation. This approach revealed that ES HSCs constantly gave rise to other HSC subsets (Figure 1D; supplemental Figure 2G), as evidenced by the equilibration of their labeling within the first year of life and revealing that the system initially indeed labeled "tip" HSCs.[22,25] Interestingly, long-term fate mapping also revealed that a considerable offset in labeling between all HSC subsets and multipotent progenitors (MPPs) persisted during 2 years of chase, implying a bottleneck of differentiation between these compartments (supplemental Figure 2G). Of note, several studies that reported the active contribution of HSC to steady-state hematopoiesis[26,27] used the *Fgd5*$^{ZsGreen:CreERT2}$ allele in combination with the *R26*$^{LSL\text{-}tdTom}$ Cre excision reporter ("Ai14"[28]) for labeling of hematopoietic stem and progenitor cells (HSPCs). However, this *R26*$^{LSL\text{-}tdTom}$ reporter has a lower activation threshold[29] than the *R26*$^{LSL\text{-}tdRFP}$ reporter used in our study, which explains the qualitative and quantitative differences in labeling of both *Fgd5*-driven fate mapping models. In sum, induction of the *Fgd5*$^{ZsGreen:CreERT2}$/*R26*$^{LSL\text{-}tdRFP}$ model results in HSC-specific labeling, which is initially enriched in ES HSCs, a population of primitive HSCs with high transplantation potential.

In addition to HSC label propagation, we determined the divisional history of HSPCs using *R26*^{rtTA}/*Col1A1*$^{H2B\text{-}GFP}$ mice (Figure 1E).[19,30] DOX administration to these mice induces ubiquitous H2B-GFP labeling. After withdrawal of the inducer, each cell division halves H2B-GFP intensity until background fluorescence levels are reached (Figure 1F).[31]

Acute inflammatory signaling under stress conditions perturbs HSC surface marker expression (supplemental Figure 3A-B) and results in contamination of the immunophenotypic HSC population with progenitor cells.[24,32] However, both reporter mouse models record either cell division (H2B-GFP dilution) or contribution of primitive HSCs (RFP label propagation) in a cumulative fashion and can be read out after the acutely perturbed hematopoietic system has returned to steady state and faithful marker expression is restored.

Myeloablation stimulates ES HSC activity

The hematopoietic system is particularly susceptible to ionizing radiation or chemotherapy, procedures that rapidly deplete cycling HSPCs and are commonly referred to as myeloablation. To investigate the contribution and proliferation of primitive HSCs in response to this perturbation, we subjected previously induced *Fgd5*$^{ZsGreen:CreERT2}$/*R26*$^{LSL\text{-}tdRFP}$ as well as *R26*^{rtTA}/*Col1A1*$^{H2B\text{-}GFP}$ reporter mice to either 2 Gy γ-radiation or 5-FU (Figure 1G-P; supplemental Figure 3C-H). To control for successful myeloablation, PB analysis 7 days later revealed a profound reduction of lymphocytes or reticulocytes (Figure 1H and I, respectively). We analyzed the composition of the lin$^-$ BM compartment 5 weeks after perturbation and found a significant reduction of HSCs and MPPs after irradiation, whereas all compartments of 5-FU–exposed BM appeared normal (Figure 1J-K). ES HSCs represent the ultimate source of propagated label and therefore serve as the reference for normalization. Myeloablation did not alter the RFP labeling of ES HSCs (Figure 1L) but strongly accelerated label propagation from ES HSCs to Sca-1^{lo} HSCs (Figure 1M; supplemental Figure 2G), which comprise more differentiated cells with low transplantation potential.[22,23,33] This label also reached progenitors and, to a lesser extent, mature blood cells. To extract the net effect of both perturbations on proliferation, we calculated the additional divisions of HSPCs in myeloablated animals compared with controls. This revealed ~3 additional divisions in HSCs, including ES HSCs in response to both perturbations (Figure 1N-O; supplemental Figure 3C-E). γ-radiation resulted in massive proliferation of MPPs and HPC-1s, thereby diluting the H2B-GFP label to the range of background controls and likely exceeding the maximum number of ~4 to 6 traceable divisions. Likewise, we calculated the net effect caused by perturbation on label propagation by subtracting the labeling of controls from the labeling of perturbed animals and plotted this data as a radar chart (Figure 1P; supplemental Figure 3F-H). Taken together, our models faithfully reported the accelerated proliferation and differentiation of ES HSCs expected upon myeloablation.[7,9,10]

Rare contribution of ES HSCs to emergency myelopoiesis

Although myeloablation proved a potent but rather artificial stimulus for ES HSC activation, inflammatory signaling resulting from infection represents a more natural hematopoietic stress

Figure 1. Fate mapping and proliferation tracking of perturbed hematopoiesis. (A) How perturbations of hematopoiesis alter contribution of a primitive HSC subset will be studied by fate mapping (red dots and arrow) and proliferation tracking (green shades and arrow). (B) *Fgd5*$^{ZsGreen:CreERT2}$/*R26*$^{LSL\text{-}tdRFP}$ mouse model for fate mapping of HSCs. (C-D) RFP labeling of HSPCs isolated from TAM-induced *Fgd5*$^{ZsGreen:CreERT2}$/*R26*$^{LSL\text{-}tdRFP}$ mice. Data from Morcos et al.[22] (C) Initial labeling frequencies of BM HSPCs 10 days after induction. (D) Labeling of total HSCs (black line) relative to ES HSCs (dotted line, 8-20 mice per time point). (E) *R26*^{rtTA}/*Col1A1*$^{H2B\text{-}GFP}$ mouse model for proliferation tracking of HSPCs. (F) Representative H2B-GFP histograms of ES HSCs isolated from 5-FU–perturbed and control mice (supplemental Figure 3C-E). (G-M) *Fgd5*$^{ZsGreen:CreERT2}$/*R26*$^{LSL\text{-}tdRFP}$ mice were TAM-induced and perturbed with either 2 Gy γ-radiation (n = 4), 5-FU (n = 5) or left untreated (n = 5). Experiment scheme (G), PB lymphocyte count 7 days after irradiation (H), PB reticulocyte numbers 7 days after 5-FU (I), and ratios of relative BM compartment sizes (% cells among total lin$^-$ BM cells) between perturbed and control (dotted line) animals (J-K) are shown. (L) Percentages of RFP$^+$ ES HSCs. (M) Fraction of RFP-labeled cells relative to ES HSCs (significant differences between untreated and either 5-FU–perturbed or irradiated mice was calculated, all comparisons between unperturbed and irradiated mice are not significant). (N-O) *R26*^{rtTA}/*Col1A1*$^{H2B\text{-}GFP}$ animals were doxycycline (DOX)–pulsed and exposed to either 2 Gy (n = 5), 5-FU (n = 5), or left untreated (n = 6). Experiment scheme (N) and numbers of additional divisions in response to perturbation (O) are shown (supplemental Figure 3C-E). (P) Transformation of data shown in panel M to visualize the net effects of myeloablation on label propagation. Mean (dark gray line) and variance (standard deviation [SD], shaded area) of control mice (n = 41 from 8 independent experiments) are shown (supplemental Figure 3F-H). CMP, common myeloid progenitor; Ery, erythrocyte; MkP, megakaryocyte progenitor; Neut, neutrophil; Plt, platelet; PMN, polymorphonuclear cell.

response. LPS is a major molecular pattern of gram-negative bacteria and triggers the expression of inflammatory cytokines via the activation of Toll-like receptor 4.[34] HSCs were reported to directly sense LPS, thereby entering the cell cycle to initiate emergency myelopoiesis, and LPS exposure in vivo caused loss of HSC transplantation potential (as previously reviewed[18]). We IP injected TAM-induced *Fgd5*$^{ZsGreen:CreERT2}$/*R26*$^{LSL\text{-}tdRFP}$ mice with a single dose of LPS and demonstrated the induction of emergency myelopoiesis by rapid recruitment of neutrophils to the injection site and increased interleukin 6 levels in PB plasma (Figure 2A-C). Unexpectedly, the massive acceleration of blood cell output upon LPS exposure was not reflected in faster label propagation from ES HSCs throughout the hematopoietic system (Figure 2D; supplemental Figure 4A-D). Although there was a slight label increase in Sca-1^{lo} HSCs, MPPs, and common myeloid progenitors, labeling of mature erythrocytes and leukocytes did not increase, demonstrating that label from ES HSCs does not reach mature myeloid cell populations even within 2 weeks after LPS-induced emergency myelopoiesis. Consistent with HSC fate mapping, LPS injection did not induce robust proliferation of early HSPCs (Figure 2E; supplemental Figure 4E). The analysis of TAM-induced fate mapping mice 24 hours after LPS injection excluded the immediate propagation of HSC-derived label to progenitors, arguing against a rapid and transient differentiation wave of primitive HSCs (supplemental Figure 4F-J).

G-CSF induces myeloid differentiation, as well as HSPC mobilization[35], and G-CSF secretion by endothelial cells in response to systemic LPS administration was identified as a key event of emergency myelopoiesis.[36] We injected previously labeled *Fgd5*$^{ZsGreen:CreERT2}$/*R26*$^{LSL\text{-}tdRFP}$ and *R26*^{rtTA}/*Col1A1*$^{H2B\text{-}GFP}$ mice for 5 consecutive days with G-CSF (Figure 2F-J; supplemental Figure 4K-N) and demonstrated mobilization of BM HSPCs to the spleen and PB (Figure 2G-H) on day 6. BM analysis conducted 47 and 25 days after G-CSF administration, respectively, uncovered a pattern of RFP label propagation (Figure 2I; supplemental Figure 4K-M) and HSPC proliferation (Figure 2J; supplemental Figure 4N), which resembled the condition in our LPS-treated animals. Specifically, we found moderately increased labeling of MPPs, but the ES HSC–derived label did not reach mature blood lineages. Again, G-CSF did not robustly stimulate additional divisions in HSCs and early progenitor cells. Because HSPC egress from the BM to the periphery is a major effect of G-CSF[35] and has previously been linked to cell proliferation,[37,38] we investigated the divisional activity of HSPCs directly after mobilization (supplemental Figure 4O-R) and detected a similar divisional history (≤1 additional division) of both mobilized and control HSCs analyzed in the BM and spleen. In contrast, the comparison of PB and BM in G-CSF–mobilized animals revealed extensive proliferation of PB HSCs (supplemental Figure 4O-P) which expressed surface markers linked to proliferation and differentiation (supplemental Figure 4Q-R), suggesting selective mobilization of less primitive HSCs into the bloodstream.

Type I IFN stimulates ES HSC divisions but little differentiation

Acute type I interferon (IFN) exposure stimulates the cell cycle entry of quiescent HSCs.[39] The synthetic double-stranded RNA analogue pI:C induces type I IFN and inflammatory cytokines via Toll-like receptor 3 activation and recapitulates key features of a viral infection. Repetitive pI:C application was shown to attrite HSC transplantation potential.[40] To induce acute or prolonged type I IFN signaling, we injected labeled fate mapping and proliferation tracking mice once or repetitively (8 times) with pI:C (Figure 2K-O; supplemental Figure 4S-Z), which resulted in an increase of PB leukocytes and reticulocytes that was persistent until 7 days after injection (Figure 2L). ES HSC label propagation was not accelerated upon a single administration of pI:C (Figure 2M; supplemental Figure 4U). Repetitive pI:C injections resulted in moderate, albeit significant, increases of labeled cells in all analyzed progenitor and mature blood cell populations, with the exception of more committed Sca-1^{lo} HSCs (Figure 2N; supplemental Figure 4Y). Importantly, pI:C robustly stimulated the mitotic activity of HSPCs in a dose-dependent manner, with at least 5 additional divisions on average in HSCs and MPPs upon repetitive pI:C application (Figure 2O; supplemental Figure 4V,Z). Taken together, acute inflammatory cytokine signaling mimicking bacterial or viral infections did not induce a robust contribution of primitive HSCs to mature blood cells (Figure 2P). Only in response to prolonged type I IFN signaling did HSPCs vigorously proliferate, but compared with myeloablation, which robustly accelerated label acquisition throughout the hierarchy, this resulted in weaker propagation of the ES HSC–derived label.

Massive loss of erythrocytes and platelets does not stimulate ES HSC output

Red blood cells (RBCs) constitute 90% of all blood cells and account for 80% to 90% of all daily renewed cells in mice and men.[41] To model acute blood loss, we injected our labeled reporter mouse models with 2 doses of PHZ (Figure 3A-E; supplemental Figure 5A-D), which destroys RBCs and potentially elicits inflammatory side effects.[42] One day after PHZ application, we observed halved hematocrit levels and RBC numbers, which equals a loss of ~7.5 × 10^9 cells per mouse, but complete regeneration was achieved by day 14 (Figure 3B-C). However, in PHZ-perturbed mice, we did not observe increased label propagation from ES HSC (Figure 2D; supplemental Figure 5A-C), and HSPC proliferation was not accelerated (Figure 3E; supplemental Figure 5D), which revealed that billions of additional RBCs were regenerated without significant input from HSCs.

Similar to RBCs, low platelet counts have potentially lethal consequences. To model acute as well as chronic thrombocytopenia, we depleted platelets by either a single or repeated injection of antiplatelet serum (Figure 3F-L; supplemental Figure 5E-L). Platelet numbers were completely recovered within 14 days after treatment (Figure 3G,I), but ES HSC–derived label propagation was neither accelerated by acute nor chronic platelet depletion (Figure 3J-K; supplemental Figure 5G,K). Antiplatelet serum dose-dependently induced less than or equal to a single additional division on average in early HSPCs (Figure 3L; supplemental Figure 5H,L), as previously reported.[43] Taken together, depletion of mature platelets and RBCs did not elicit a substantial contribution of primitive HSCs to mature blood cells (Figure 3M).

Discussion

Primitive HSCs with high transplantation potential are regarded as a reserve population that directly fuels emergency

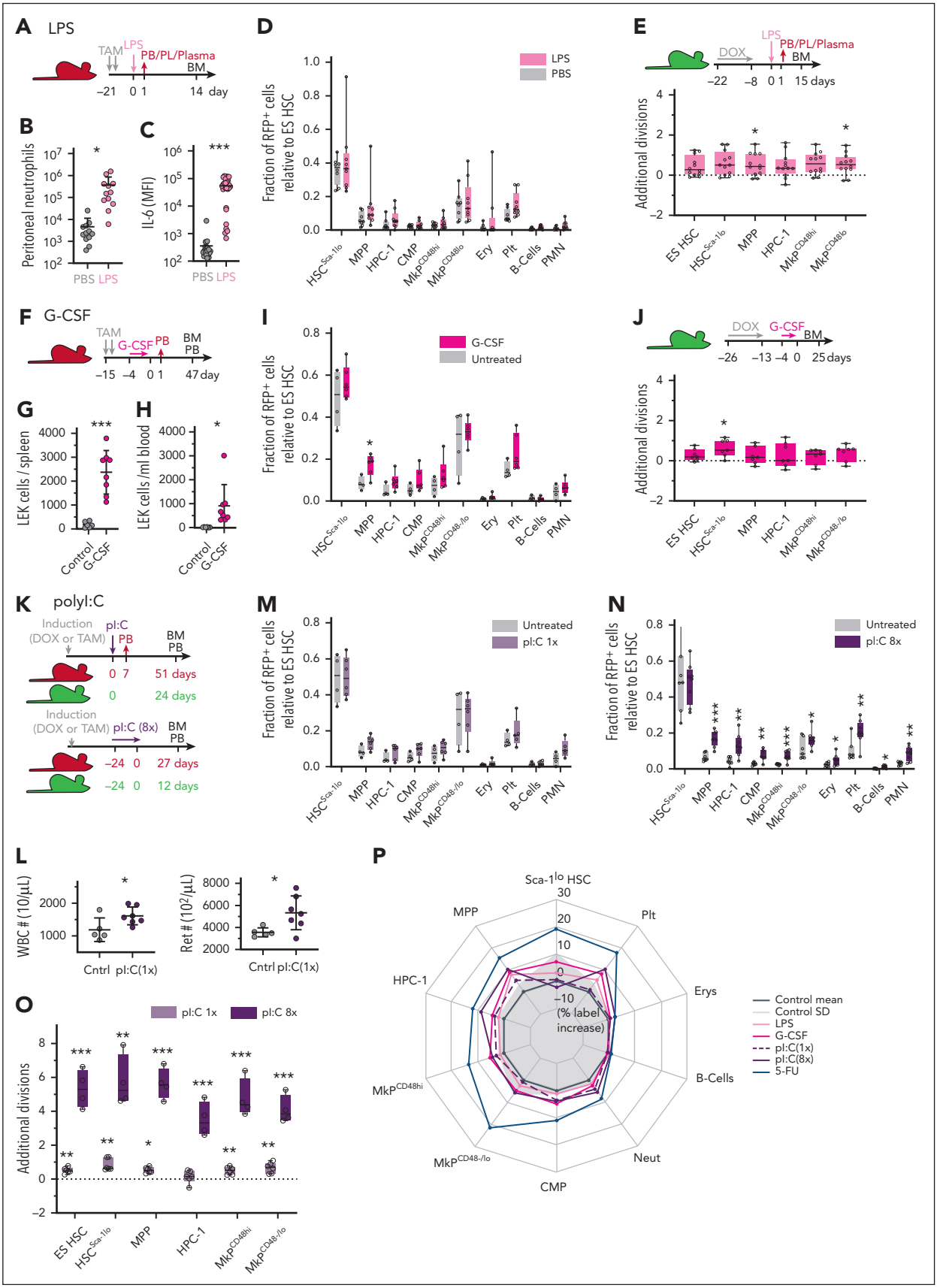

Figure 2. Limited contribution of HSCs to emergency myelopoiesis and type I IFN stimulation. (A-D) *Fgd5*$^{ZsGreen:CreERT2}$/*R26*$^{LSL-tdRFP}$ mice were TAM-induced and injected with LPS (n = 8) or PBS (n = 12). (B) Neutrophil count in the peritoneal cavity 24 hours after LPS/PBS injection. (C) Plasma levels of interleukin 6 (IL-6) 90 minutes after LPS/PBS injection. (D) Fraction of RFP-labeled cells (relative to ES HSCs) between LPS and saline-treated animals. Data from 2 independent experiments. (E) Labeled *R26*^{rtTA}/*Col1A1*$^{H2B-GFP}$ animals were

hematopoiesis.[15-17] We investigated the contribution of these cells to hematopoietic stress responses under native conditions and found that the flux from ES HSCs to their immediate progeny did only marginally increase in response to perturbations, and did not reach more distant populations, thereby raising the question of how hematopoietic stress responses are hierarchically organized.

Transiently boosted output rates from ES HSCs during emergency can be captured by fate mapping, as they accelerate label equilibration between ES HSCs and progenitors and result in permanently altered labeling of ES HSC progeny. Our *Fgd5*$^{ZsGreen:CreERT2}$/*R26*$^{LSL\text{-}tdRFP}$ fate mapping model labels ~10% of ES HSCs, which then serve as a proxy for the entire population. This assumption is substantiated by the following observations: (1) the labeling of ES HSCs and total immunophenotypic HSC completely equilibrated starting from 1 year after induction (Figure 1D), which must result from similar contribution of labeled and unlabeled ES HSCs; (2) this label steadily propagated in a linear fashion to all mature blood cell lineages; and (3) most of the long-term transplantation potential is confined to ES HSCs and similar in labeled and unlabeled ES HSCs (supplemental Figure 2E-F). How blood regeneration can evoke increased input from HSCs is exemplified by myeloablation, which represents a severe, potentially life-threatening perturbation and robustly accelerated HSPC proliferation, as well as the propagation of the ES HSC–derived label. In addition, this demonstrated the feasibility of both H2B-GFP– and Cre/lox*P*-based tracking strategies and argued against previously reported adverse effects of label induction.[44-46] Of note, even in response to myeloablative irradiation or chemotherapy, only a minority of ES HSCs differentiated into their immediate progeny (Figure 1M). Likewise, upon transplantation, HSCs on their own are insufficient to ensure the short-term survival of the myeloablated host, and erythromyeloid progenitors were shown to be crucial for initial radioprotection until HSCs provide long-term repopulation.[47] Hence, HSCs are not able to rapidly generate sufficient numbers of mature blood cells, despite their superior self-renewal potential.

In contrast to myeloablation, primitive HSCs only marginally contributed to mature blood cell production under conditions mimicking an acute bacterial or viral infection. Importantly, ES HSC–derived label did not reach mature myeloid cells faster upon LPS- or G-CSF–induced perturbation, demonstrating that this stress response was achieved without direct input from primitive HSCs. It is conceivable that less primitive HSC subsets (eg, Sca-1^{lo} HSCs) respond to emergency myelopoiesis independently from ES HSCs. Although our fate mapping mouse model preferentially labels ES HSCs, we still observe considerable labeling of Sca-1^{lo} HSCs (three- to fivefold higher than in MPPs). Therefore, a significant contribution of non–ES HSC would be traceable, but we found that the labeling offset between HSC subsets and MPPs resisted all perturbations, implying that all HSCs did not considerably increase their output and regeneration was initiated by MPPs, as recently demonstrated.[48]

Hematopoietic perturbations could result in a rapid and direct differentiation of HSCs into short-lived progeny without considerable self-renewal. Our fate mapping model may not capture transient HSC progeny or input emanating from a few HSCs. Such behavior would assume that stress-induced HSC progeny has fundamentally altered differentiation and self-renewal properties at all hierarchical levels. However, our fate mapping experiments revealed a stable and increased labeling of short-lived granulocytes and platelets 5 weeks after myeloablation (Figure 1M), arguing for similar properties of HSC progeny under stress and homeostatic conditions. Moreover, BM analysis 24 hours after LPS perturbation did not reveal a label increase in myeloid progenitors, providing evidence against a transient wave of mature myeloid progeny originating directly from HSCs (supplemental Figure 4F-J).

Although acute LPS or G-CSF stimulation provoked only minimal cell division of HSPCs, type I IFN exposure robustly induced proliferation, as previously reported.[39,40] Given the massive proliferation of HSPCs in response to escalating doses of pI:C, this protocol induced significant but surprisingly little differentiation of labeled ES HSCs. We speculate that a massive type I IFN response provoked cell death in HSPCs and that proliferation of residual cells compensated for this loss without simultaneously increasing the differentiation flux from ES HSCs. Indeed, exaggerated type I IFN was shown to induce cell death.[49] However, HSCs were reported to be refractory to its destructive effects.[50,51] This may explain why chronic pI:C perturbation resulted in only marginally higher RFP label propagation than the acute pI:C protocol.

Our finding that primitive HSCs participate rarely, if at all, in hematopoietic stress responses contrasts with the frequent observation that acute infection and inflammation stimulate cell cycle entry and profoundly reduce HSC transplantation potential (as previously reviewed[18]). This phenomenon has usually been linked to attrition of HSC during stress responses[52] and can be exacerbated further by applying chronic or severe perturbation protocols. Our results now show that primitive HSCs with high transplantation potential do not robustly proliferate or differentiate in response to acute inflammation. This discrepancy might be explained by acute inflammatory signaling confounding surface marker expression and resulting in contamination of the HSC population with cycling progenitors. Accordingly, cell cycle entry as well as attrition of HSC transplantation potential in response to inflammation were not observed when HSCs were defined by Fgd5,[24,53] CD86,[32] or EPCR expression.[53]

Figure 2 (continued) IP injected with LPS (n = 14) or PBS (n = 13) and the average number of additional divisions in response to LPS was determined. Data from 2 independent experiments. (F-J) *Fgd5*$^{ZsGreen:CreERT2}$/*R26*$^{LSL\text{-}tdRFP}$ (in panels F and I, n = 4-6 per condition) and *R26*^{rtTA}/*Col1A1*$^{H2B\text{-}GFP}$ (in panels G, H, and J, n = 4-7 per condition) mice were subcutaneously injected with G-CSF or PBS for 5 consecutive days. Numbers of LEK HSPCs in spleen (G) or PB (H) of *R26*^{rtTA}/*Col1A1*$^{H2B\text{-}GFP}$ animals on d6. (I) Fraction of RFP-labeled cells (relative to ES HSCs). (J) Average number of additional divisions in response to G-CSF. (K-O) *Fgd5*$^{ZsGreen:CreERT2}$/*R26*$^{LSL\text{-}tdRFP}$ (in panels K-N, n = 4-8 per condition) and *R26*^{rtTA}/*Col1A1*$^{H2B\text{-}GFP}$ (in panel O, n = 4-7 per condition) mice were IP injected with pI:C or PBS following either a single (once) or repetitive (8 times) administration protocol. (L) PB leukocyte and reticulocyte numbers 7 days after 1 time pI:C. (M-N) Fraction of RFP-labeled cells (relative to ES HSCs). (O) Average number of additional divisions in response to pI:C. (P) Net effects of LPS, G-CSF, or pI:C perturbation on RFP label propagation (% label increase relative to ES HSCs; transformation and display of data as in Figure 1P). MFI, mean fluorescence intensity; PL, peritoneal lavage.

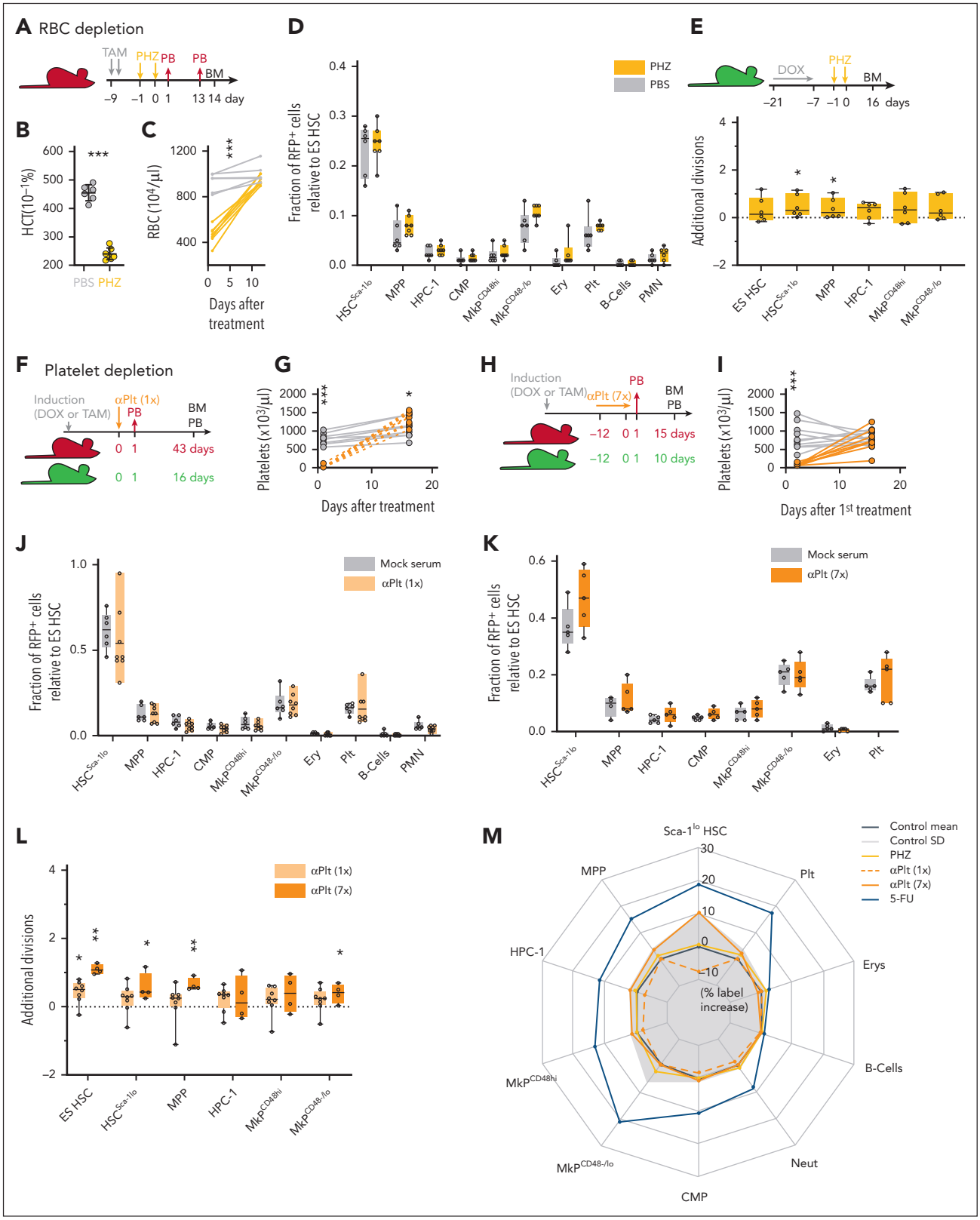

Figure 3. Limited contribution of HSCs to recovery from blood loss. (A-E) *Fgd5*$^{ZsGreen:CreERT2}$/*R26*$^{LSL-tdRFP}$ (in panels A-D, n = 6-7 per condition) and *R26*^{rtTA}/*Col1A1*$^{H2B-GFP}$ (in panel E, n = 6-7 per condition) mice were IP injected with phenylhydrazine (PHZ) or PBS. Hematocrit (HCT) 24 hours after PHZ application (B) and PB RBC numbers (C) are shown. (D) Fraction of RFP-labeled cells (relative to ES HSCs). (E) Average number of additional divisions in response to PHZ. (F-L) *Fgd5*$^{ZsGreen:CreERT2}$/*R26*$^{LSL-tdRFP}$ (in panels F-K, n = 4-8 per condition) and *R26*^{rtTA}/*Col1A1*$^{H2B-GFP}$ (in panel L, n = 4-8 per condition) mice were treated with antiplatelet (αPlt) serum or control serum following a single (once in panels F-G, J, and L) or repetitive (7 times in panels H-I and K-L) application protocol. (G-I) Platelet numbers in PB. (J-K) Fraction of RFP-labeled cells (relative to ES HSCs). (L) Average number of additional divisions in response to platelet depletion. (M) Net effects of RBC or platelet depletion on RFP label propagation (% label increase relative to ES HSCs; transformation and display of data as in Figure 1P).

The main regenerative burden of the hematopoietic system under steady-state conditions is the production of RBCs and platelets.[1] Interestingly, the rapid recovery after a severe and potentially life-threatening reduction of either cell type occurred without significant ES HSC input. RBCs can solely be replaced by a massive proliferation of progenitor cells, whereas thousands of platelets are generated by a single megakaryocyte. Accordingly, the direct differentiation of HSCs into megakaryocytes is well documented.[22,54-56] Both amplification strategies, however, might be too slow for emergency responses emanating from the relatively small HSC population. To rapidly put out 10^9 RBCs, 10^4 HSCs would have to simultaneously undergo massive expansion and maturation within several days. Similarly, the process of endoreplication in nascent megakaryocytes might take too long to boost emergency thrombopoiesis. Reports of an inflammation-induced HSC-like megakaryocyte progenitor population could result from omitting Sca-1 from the HSPC gating strategy.[57] Thus, these cells could actually correspond to CD48$^{-/lo}$ megakaryocyte progenitors,[22] which immunophenotypically resemble HSCs except for lacking Sca-1 and EPCR expression.

Our results argue that primitive HSCs do not represent a reserve population for commonly encountered hematopoietic challenges, such as blood loss and inflammation, and only chronic inflammatory or myeloablative hematopoietic stress warrants increased HSC input. Instead, we speculate that primitive HSCs slowly differentiate or "trickle-down" to constantly replenish and rejuvenate progenitor pools at a very low rate, whereas acute stress conditions only mildly amplify this process. Consequently, many hematopoietic perturbations must be primarily compensated by increased self-renewal and contribution of progenitors. Given the underappreciated self-renewal capacity and longevity of MPPs under native conditions,[12] these cells are in principle well equipped to compensate hematopoietic perturbations independent of HSCs. The fact that only a minor fraction of humans ever suffer from BM failure in spite of the lifelong recurrence of infections also argues for a reevaluation of the concept of stress-induced HSC attrition.

Acknowledgments

The authors thank Christa Haase, Livia Schulze, and Luisa Röbisch for expert technical assistance, and Hans-Reimer Rodewald and Thomas Höfer for sharing of unpublished data.

This work was supported by funding from the German Research Council (DFG, GE3038/1-1) (A.G.) and (TR237 [B17]) (A.R.).

Authorship

Contribution: C.M.M. performed experiments with help from N.D. and M.C.; T.G. provided methodology; A.G. conceived and supervised the study; A.G. and C.M.M. wrote the paper; and A.R. revised the manuscript.

Conflict-of-interest disclosure: The authors declare no competing financial interests.

ORCID profiles: C.M.M., 0000-0002-4823-7598; N.D., 0000-0002-5070-7018; M.C., 0000-0002-9299-5353; T.G., 0000-0002-2582-1417; A.R., 0000-0003-1806-6158; A.G., 0000-0003-4680-4920.

Correspondence: Alexander Gerbaulet, Institute for Immunology, Medical Faculty, TU Dresden, Fetscherstraße 74, 01307 Dresden, Germany; email: alexander.gerbaulet@tu-dresden.de.

Footnotes

Submitted 28 November 2022; accepted 1 February 2023; prepublished online on *Blood* First Edition 14 February 2023. https://doi.org/10.1182/blood.2022018996.

Data are available on request from the corresponding author, Alexander Gerbaulet (alexander.gerbaulet@tu-dresden.de).

The online version of this article contains a data supplement.

There is a *Blood* Commentary on this article in this issue.

The publication costs of this article were defrayed in part by page charge payment. Therefore, and solely to indicate this fact, this article is hereby marked "advertisement" in accordance with 18 USC section 1734.

REFERENCES

1. Cosgrove J, Hustin LSP, de Boer RJ, Perié L. Hematopoiesis in numbers. *Trends Immunol*. 2021;42(12):1100-1112.
2. Thomas ED, Lochte HL, Lu WC, Ferrebee JW. Intravenous infusion of bone marrow in patients receiving radiation and chemotherapy. *N Engl J Med*. 1957;257(11):491-496.
3. Purton LE, Scadden DT. Limiting factors in murine hematopoietic stem cell assays. *Cell Stem Cell*. 2007;1(3):263-270.
4. Rodriguez-Fraticelli AE, Weinreb C, Wang S-W, et al. Single-cell lineage tracing unveils a role for TCF15 in haematopoiesis. *Nature*. 2020;583(7817):585-589.
5. Naik SH, Perié L, Swart E, et al. Diverse and heritable lineage imprinting of early haematopoietic progenitors. *Nature*. 2013;496(7444):229-232.
6. Sun J, Ramos A, Chapman B, et al. Clonal dynamics of native haematopoiesis. *Nature*. 2014;514(7522):322-327.
7. Busch K, Klapproth K, Barile M, et al. Fundamental properties of unperturbed haematopoiesis from stem cells in vivo. *Nature*. 2015;518(7540):542-546.
8. Pei W, Feyerabend TB, Rössler J, et al. Polylox barcoding reveals haematopoietic stem cell fates realized in vivo. *Nature*. 2017;548(7668):456-460.
9. Bowling S, Sritharan D, Osorio FG, et al. An engineered CRISPR-Cas9 mouse line for simultaneous readout of lineage histories and gene expression profiles in single cells. *Cell*. 2020;181(6):1410-1422.e27.
10. Wilson A, Laurenti E, Oser G, et al. Hematopoietic stem cells reversibly switch from dormancy to self-renewal during homeostasis and repair. *Cell*. 2008;135(6):1118-1129.
11. Visser JW, Bol SJ, van den Engh G. Characterization and enrichment of murine hemopoietic stem cells by fluorescence activated cell sorting. *Exp Hematol*. 1981;9(6):644-655.
12. Patel SH, Christodoulou C, Weinreb C, et al. Lifelong multilineage contribution by embryonic-born blood progenitors. *Nature*. 2022;606(7915):747-753.
13. Schoedel KB, Morcos MNF, Zerjatke T, et al. The bulk of the hematopoietic stem cell population is dispensable for murine steady-state and stress hematopoiesis. *Blood*. 2016;128(19):2285-2296.
14. Sheikh BN, Yang Y, Schreuder J, et al. MOZ (KAT6A) is essential for the maintenance of classically defined adult hematopoietic stem cells. *Blood*. 2016;128(19):2307-2318.
15. Takizawa H, Boettcher S, Manz MG. Demand-adapted regulation of early hematopoiesis in infection and inflammation. *Blood*. 2012;119(13):2991-3002.
16. King KY, Goodell MA. Inflammatory modulation of HSCs: viewing the HSC as a foundation for the immune response. *Nat Rev Immunol*. 2011;11(10):685-692.

17. Trumpp A, Essers M, Wilson A. Awakening dormant haematopoietic stem cells. *Nat Rev Immunol*. 2010;10(3):201-209.

18. Caiado F, Pietras EM, Manz MG. Inflammation as a regulator of hematopoietic stem cell function in disease, aging, and clonal selection. *J Exp Med*. 2021;218(7): e20201541.

19. Foudi A, Hochedlinger K, Van Buren D, et al. Analysis of histone 2B-GFP retention reveals slowly cycling hematopoietic stem cells. *Nat Biotechnol*. 2009;27(1):84-90.

20. Luche H, Weber O, Nageswara Rao T, Blum C, Fehling HJ. Faithful activation of an extra bright red fluorescent protein in "knock in" Cre reporter mice ideally suited for lineage tracing studies. *Eur J Immunol*. 2007; 37(1):43-53.

21. Gazit R, Mandal PK, Ebina W, et al. Fgd5 identifies hematopoietic stem cells in the murine bone marrow. *J Exp Med*. 2014; 211(7):1315-1331.

22. Morcos MNF, Li C, Munz CM, et al. Fate mapping of hematopoietic stem cells reveals two pathways of native thrombopoiesis. *Nat Commun*. 2022;13(1):4504.

23. Morcos MNF, Schoedel KB, Hoppe A, et al. SCA-1 Expression level identifies quiescent hematopoietic stem and progenitor cells. *Stem Cell Rep*. 2017;8(6):1472-1478.

24. Bujanover N, Goldstein O, Greenshpan Y, et al. Identification of immune-activated hematopoietic stem cells. *Leukemia*. 2018; 32(9):2016-2020.

25. Takahashi M, Barile M, Chapple RH, et al. Reconciling Flux experiments for quantitative modeling of normal and malignant hematopoietic stem/progenitor dynamics. *Stem Cell Rep*. 2021;16(4):741-753.

26. Säwen P, Eldeeb M, Erlandsson E, et al. Murine HSCs contribute actively to native hematopoiesis but with reduced differentiation capacity upon aging. *Elife*. 2018;7:e41258.

27. Chapple RH, Tseng Y-J, Hu T, et al. Lineage tracing of murine adult hematopoietic stem cells reveals active contribution to steady-state hematopoiesis. *Blood Adv*. 2018;2(11): 1220-1228.

28. Madisen L, Zwingman TA, Sunkin SM, et al. A robust and high-throughput Cre reporting and characterization system for the whole mouse brain. *Nat Neurosci*. 2010;13(1): 133-140.

29. Álvarez-Aznar A, Martínez-Corral I, Daubel N, Betsholtz C, Mäkinen T, Gaengel K. Tamoxifen-independent recombination of reporter genes limits lineage tracing and mosaic analysis using CreERT2 lines. *Transgenic Res*. 2020;29(1):53-68.

30. Kanda T, Sullivan KF, Wahl GM. Histone-GFP fusion protein enables sensitive analysis of chromosome dynamics in living mammalian cells. *Curr Biol*. 1998;8(7):377-385.

31. Morcos MNF, Zerjatke T, Glauche I, et al. Continuous mitotic activity of primitive hematopoietic stem cells in adult mice. *J Exp Med*. 2020;217(6):e20191284.

32. Kanayama M, Izumi Y, Yamauchi Y, et al. CD86-based analysis enables observation of bona fide hematopoietic responses. *Blood*. 2020;136(10):1144-1154.

33. Säwén P, Lang S, Mandal P, Rossi DJ, Soneji S, Bryder D. Mitotic history reveals distinct stem cell populations and their contributions to hematopoiesis. *Cell Rep*. 2016;14(12):2809-2818.

34. Beutler BA. TLRs and innate immunity. *Blood*. 2009;113(7):1399-1407.

35. Greenbaum AM, Link DC. Mechanisms of G-CSF-mediated hematopoietic stem and progenitor mobilization. *Leukemia*. 2011; 25(2):211-217.

36. Boettcher S, Gerosa RC, Radpour R, et al. Endothelial cells translate pathogen signals into G-CSF–driven emergency granulopoiesis. *Blood*. 2014;124(9): 1393-1403.

37. Bernitz JM, Daniel MG, Fstkchyan YS, Moore K. Granulocyte colony-stimulating factor mobilizes dormant hematopoietic stem cells without proliferation in mice. *Blood*. 2017;129(14):1901-1912.

38. Morrison SJ, Wright DE, Weissman IL. Cyclophosphamide/granulocyte colony-stimulating factor induces hematopoietic stem cells to proliferate prior to mobilization. *Proc Natl Acad Sci U S A*. 1997;94(5):1908-1913.

39. Essers MAG, Offner S, Blanco-Bose WE, et al. IFNalpha activates dormant haematopoietic stem cells in vivo. *Nature*. 2009;458(7240): 904-908.

40. Bogeska R, Mikecin A-M, Kaschutnig P, et al. Inflammatory exposure drives long-lived impairment of hematopoietic stem cell self-renewal activity and accelerated aging. *Cell Stem Cell*. 2022;29(8):1273-1284.e8.

41. Sender R, Milo R. The distribution of cellular turnover in the human body. *Nat Med*. 2021; 27(1):45-48.

42. Dutra FF, Alves LS, Rodrigues D, et al. Hemolysis-induced lethality involves inflammasome activation by heme. *Proc Natl Acad Sci U S A*. 2014;111(39):E4110-E4118.

43. Ramasz B, Krüger A, Reinhardt J, et al. Hematopoietic stem cell response to acute thrombocytopenia requires signaling through distinct receptor tyrosine kinases. *Blood*. 2019;134(13):1046-1058.

44. Sanchez-Aguilera A, Arranz L, Martin-Perez D, et al. Estrogen signaling selectively induces apoptosis of hematopoietic progenitors and myeloid neoplasms without harming steady-state hematopoiesis. *Cell Stem Cell*. 2014; 15(6):791-804.

45. Ito S, Magalska A, Alcaraz-Iborra M, et al. Loss of neuronal 3D chromatin organization causes transcriptional and behavioural deficits related to serotonergic dysfunction. *Nat Commun*. 2014;5(1):4450.

46. Hameyer D, Loonstra A, Eshkind L, et al. Toxicity of ligand-dependent Cre recombinases and generation of a conditional Cre deleter mouse allowing mosaic recombination in peripheral tissues. *Physiol Genomics*. 2007;31(1):32-41.

47. Na Nakorn T, Traver D, Weissman IL, Akashi K. Myeloerythroid-restricted progenitors are sufficient to confer radioprotection and provide the majority of day 8 CFU-S. *J Clin Invest*. 2002;109(12): 1579-1585.

48. Fanti A-K, Busch K, Greco A, et al. Flt3- and Tie2-Cre tracing identifies regeneration in sepsis from multipotent progenitors but not hematopoietic stem cells. *Cell Stem Cell*. 2023;30(2):207-218.e7.

49. Chawla-Sarkar M, Lindner DJ, Liu YF, et al. Apoptosis and interferons: role of interferon-stimulated genes as mediators of apoptosis. *Apoptosis*. 2003;8(3):237-249.

50. Wu X, Dao Thi VL, Huang Y, et al. Intrinsic immunity shapes viral resistance of stem cells. *Cell*. 2018;172(3):423-438.e25.

51. Pietras EM, Lakshminarasimhan R, Techner J-M, et al. Re-entry into quiescence protects hematopoietic stem cells from the killing effect of chronic exposure to type I interferons. *J Exp Med*. 2014;211(2): 245-262.

52. Walter D, Lier A, Geiselhart A, et al. Exit from dormancy provokes DNA-damage-induced attrition in haematopoietic stem cells. *Nature*. 2015;520(7548):549-552.

53. Rabe JL, Hernandez G, Chavez JS, Mills TS, Nerlov C, Pietras EM. CD34 and EPCR coordinately enrich functional murine hematopoietic stem cells under normal and inflammatory conditions. *Exp Hematol*. 2020; 81:1-15.e6.

54. Rodriguez-Fraticelli AE, Wolock SL, Weinreb CS, et al. Clonal analysis of lineage fate in native haematopoiesis. *Nature*. 2018; 553(7687):212-216.

55. Yamamoto R, Morita Y, Ooehara J, et al. Clonal Analysis unveils self-renewing lineage-restricted progenitors generated directly from hematopoietic stem cells. *Cell*. 2013; 154(5):1112-1126.

56. Grinenko T, Eugster A, Thielecke L, et al. Hematopoietic stem cells can differentiate into restricted myeloid progenitors before cell division in mice. *Nat Commun*. 2018;9(1): 1898.

57. Haas S, Hansson J, Klimmeck D, et al. Inflammation-Induced emergency megakaryopoiesis driven by hematopoietic stem cell-like megakaryocyte progenitors. *Cell Stem Cell*. 2015;17(4):422-434.